

## ADIABATIC SHEAR BANDING IN ELASTIC-VISCOPLASTIC NONPOLAR AND DIPOLAR MATERIALS

R.C. BATRA and C.H. KIM

University of Missouri-Rolla

**Abstract**—Simple shearing deformations of a block made of an elastic-viscoplastic material are studied. The material of the block is presumed to exhibit strain hardening, strain-rate hardening and thermal softening. The effect of modeling the material of the block as a dipolar material in which the strain gradient is also taken as an independent variable has been investigated. The uniform fields of temperature and shear stress in the block are perturbed by superimposing a temperature bump at the center of the block, and the resulting initial-boundary-value problem is solved by the Galerkin-Gear method. It is found that for simple materials as the shear stress within the region of localization begins to collapse, an unloading elastic shear wave emanates outwards from the edges of the shear band. For dipolar materials, the localization of the deformation is considerably delayed as compared to that for nonpolar materials, the shear stress does not collapse suddenly but decreases gradually, there is no unloading wave traveling outwards from the edges of the band, and the region of localized deformation is wider as compared to that for nonpolar materials.

### I. INTRODUCTION

Since the time ZENER and HOLLOMON [1944] observed 32  $\mu\text{m}$  wide shear bands in a steel plate punched by a standard die and estimated the maximum strain in the band to be 100, there has been a considerable amount of research done in understanding factors that influence the initiation and growth of adiabatic shear bands. ROGERS [1979,1983] has vividly summarized in his review articles the work done on adiabatic shear banding until 1982. References to some of the other experimental, analytical and numerical studies may be found in CLIFTON *et al.* [1984] and BATRA [1987].

Recently, MARCHAND and DUFFY [1988] have given a detailed history of the temperature and strain fields within a band. Their experimental observations confirm the earlier prediction by WRIGHT and WALTER [1987] that the shear stress within a band collapses as the deformation localizes. Wright and Walter gave details of the shear band morphology for a rigid viscoplastic material. Herein we also account for (i) the material elasticity, (ii) work hardening, and (iii) the consideration of strain gradient as an independent variable. For simple materials, it is found that as the deformation begins to localize the shear stress collapses and an unloading elastic shear wave travels outwards from the region of severe deformation. For dipolar materials the shear stress drops gradually and there is no unloading elastic wave observed. The region of severe deformation is wider for dipolar materials as compared to that for nonpolar materials.

Whereas CLIFTON *et al.* [1984], WRIGHT and BATRA [1985], and BATRA [1987] accounted for the effect of material elasticity, their calculations were not carried far enough in time to see what effect, if any, the material elasticity has once a shear band has formed. Wright and Batra, and Batra used, respectively, the forward-difference method and the Crank-Nicolson method to integrate the ordinary differential equations obtained by applying the Galerkin approximation to the governing partial differential

equations. Both these methods became unstable once the deformation started to localize. The Gear method used by WRIGHT and WALTER [1987] and also employed here enables us to study the details of the deformation within the severely deformed region. The results presented here should help to better understand the mechanics of the shear band formation.

## II. FORMULATION OF THE PROBLEM

Equations governing the thermomechanical deformations of a block of material undergoing simple shearing motion are:

$$\text{The balance of linear momentum, } \rho \ddot{u} = (s - \sigma_{,y})_{,y}, \quad (1)$$

$$\text{The balance of internal energy, } \rho \dot{e} = -q_{,y} + sv_{,y} + \sigma v_{,yy}. \quad (2)$$

Here  $\rho$  is the mass density,  $u$  is the  $x$ -displacement and  $v$  the  $x$ -velocity of a material particle,  $s$  is the shear stress,  $\sigma$  is the dipolar stress associated with the kinematic variable  $u_{,yy}$ ,  $q$  is the heat flux,  $e$  is the specific internal energy, a comma followed by  $y$  implies partial differentiation with respect to  $y$ , and a superimposed dot signifies material time differentiation. For the sake of completeness and brevity, we give only the equations which are absolutely necessary for our work. Detailed discussions of these equations and those given below may be found in GREEN, MCINNIS and NAGHDI [1968] and WRIGHT and BATRA [1987].

COLEMAN and HODGON [1985] have developed a theory of shear banding in which the shear yield stress depends upon the accumulated shear strain  $\bar{\gamma}$  and its second spatial gradient. For monotonic loading the accumulated shear strain equals the present value of the shear strain  $\gamma$ . Previous numerical (e.g., BATRA [1987]) and experimental work (MARCHAND & DUFFY [1988]) on the adiabatic shearing problem indicates that peak strain gradients are of the order of  $10^7$  per meter. It seems reasonable to assume that such a deforming region will experience a force which opposes these sharp gradients of  $\gamma$ . COLEMAN and HODGON [1985] introduced such a force into the theory by adding, to the expression for the stress in the classical flow rule, a term linear in the second spatial derivative of  $\gamma$ . Here we account for this force by taking the first spatial derivative of  $\gamma$  as a kinematic variable and account for the effects of the associated dipolar stress  $\sigma$  on the deformations of the body.

We presume that the shear strain  $\gamma$  and the shear strain gradient  $d$  have additive decompositions into elastic ( $\gamma_e, d_e$ ) and plastic ( $\gamma_p, d_p$ ) parts. That is,

$$\gamma \equiv u_{,y} = \gamma_e + \gamma_p, \quad (3)$$

$$d \equiv u_{,yy} = d_e + d_p. \quad (4)$$

For the constitutive relations we take

$$q = -k\theta_{,y}, \quad (5)$$

$$\dot{s} = \mu \dot{\gamma}_e, \quad (6)$$

$$\dot{\sigma} = \nu \dot{d}_e, \quad (7)$$

$$\dot{\epsilon} = c\dot{\theta} + s\dot{\gamma}_e + \sigma\dot{d}_e, \quad (8)$$

$$\dot{\gamma}_p = \Lambda s, \quad (9)$$

$$\dot{d}_p = \frac{\Lambda}{\ell_1^2} \sigma, \quad (10)$$

where  $k$  is the thermal conductivity,  $c$  the specific heat,  $\theta$  the change in the temperature of a material particle from its temperature in the reference configuration,  $\mu$  is the shear modulus,  $\nu$  is the modulus associated with the dipolar effects,  $\ell_1$  is a material characteristic length, and  $\Lambda = \Lambda(s, \sigma, \gamma_p, d_p)$  is positive for plastic deformations and equals zero when the deformations are elastic. All of the material parameters  $\mu$ ,  $k$ ,  $c$  and  $\nu$  are assumed to be constants.

To decide whether the ensuing deformations are elastic or plastic, we presume that there exists a loading function

$$f(s, \sigma, \dot{\gamma}_p, \dot{d}_p, \theta) = \kappa(\gamma_p, d_p) \quad (11)$$

such that for all positive  $\lambda$  and real numbers  $a$  and  $b$ ,

$$\frac{\partial f}{\partial \lambda}(s, \sigma, \lambda a, \lambda b, \theta) < 0. \quad (12)$$

The function  $\kappa$  on the right-hand side of eqn (11) describes the work hardening of the material. The condition (12) ensures that the equation

$$f\left(s, \sigma, \Lambda s, \frac{\Lambda}{\ell_1^2} \sigma, \theta\right) = \kappa(\gamma_p, d_p) \quad (13)$$

has a unique solution for  $\Lambda$ . We make the following choices for  $f$  and  $\kappa$

$$f = \left(s^2 + \frac{\sigma^2}{\ell_1^2}\right)^{1/2} \frac{1}{(1 - a\theta)} (1 + b(\dot{\gamma}_p^2 + \ell_2^2 \dot{d}_p^2)^{1/2})^{-m}, \quad (14)$$

$$\kappa = \kappa_0 \left(1 + \frac{\psi}{\psi_0}\right)^n, \quad (15)$$

$$\kappa \dot{\psi} = s\dot{\gamma}_p + \sigma\dot{d}_p. \quad (16)$$

The parameter  $a$  describes the thermal softening of the material,  $b$  and  $m$  its strain-rate hardening,  $\psi_0$  and  $n$  characterize its work hardening, and  $\kappa_0$  is the yield stress in a quasi-static isothermal test. The parameter  $\psi$  introduced through eqns (15) and (16) may be thought of as an internal variable. It describes the effect of the history of the deformation on the current value of the yield stress in a quasi-static and isothermal test. It is referred to as the work hardening parameter below.

Substitution from (14), (15), (9) and (10) into (11) yields

$$\left(s^2 + \frac{\sigma^2}{\ell_1^2}\right)^{1/2} = \kappa_0 \left(1 + \frac{\psi}{\psi_0}\right)^n (1 - a\theta) \left(1 + b\Lambda \left(s^2 + \frac{\ell_2^2}{\ell_1^4} \sigma^2\right)^{1/2}\right)^m \quad (17)$$

which is to be solved for  $\Lambda$  when plastic deformation is occurring; otherwise  $\Lambda$  is zero. The constitutive eqn (17) is a simple variation of the "overstress" idea, due to MALVERN [1984], where the overstress in the present case is obtained through the use of a multiplicative factor rather than an additive one. When the dipolar effects are neglected and the material is presumed to be viscoplastic without any yield surface, then eqn (17) reduces to LITONSKI'S [1977] constitutive relation.

Before discussing the initial and boundary conditions, we nondimensionalize the variables as follows:

$$\begin{aligned} y &= H\bar{y}, \quad u = H\bar{u}, \quad \ell_1 = \bar{\ell}_1 H, \quad \ell_2 = \bar{\ell}_2 H, \quad \gamma = \bar{\gamma}, \quad d = \bar{d}/H, \quad \psi = \bar{\psi}, \\ s &= \kappa_0 \bar{s}, \quad \sigma = \kappa_0 \ell_2 \bar{\sigma}, \quad \kappa = \kappa_0 \bar{\kappa}, \quad \Lambda = \frac{\dot{\gamma}_0}{\kappa_0} \bar{\Lambda}, \quad t = \frac{\bar{t}}{\dot{\gamma}_0}, \quad \theta = \theta_0 \bar{\theta}, \\ \frac{\rho H^2 \dot{\gamma}_0^2}{\kappa_0} &= \bar{\rho}, \quad \frac{k}{\rho c \dot{\gamma}_0 H^2} = \bar{k}, \quad a\theta_0 = \bar{a}, \quad b\dot{\gamma}_0 = \bar{b}, \quad \theta_0 \equiv \frac{\kappa_0}{\rho c}, \\ \bar{\mu}\kappa_0 &= \mu, \quad \bar{\nu}\kappa_0 \ell_3^2 = \nu, \quad \ell_3 = \bar{\ell}_3 H. \end{aligned} \quad (18)$$

Here  $2H$  is the height of the block,  $\dot{\gamma}_0$  is the average strain-rate,  $\ell_3$  is a material characteristic length, and the overbar indicates the nondimensional quantity. Below we drop the overbars and give a summary of the equations in terms of nondimensional variables.

$$\rho \dot{v} = (s - \ell \sigma_{,y})_{,y}, \quad (19)$$

$$\dot{\theta} = k\theta_{,yy} + \Lambda(s^2 + \sigma^2), \quad (20)$$

$$\dot{s} = \mu(v_{,y} - \Lambda s), \quad (21)$$

$$\dot{\sigma} = \mu \ell \left( v_{,yy} - \frac{\Lambda \sigma}{\ell} \right), \quad (22)$$

$$\dot{\psi} = \frac{\Lambda(s^2 + \sigma^2)}{\left(1 + \frac{\psi}{\psi_0}\right)^n}, \quad (23)$$

$$\Lambda = \max \left\{ 0, \left( \left( \frac{(s^2 + \sigma^2)^{1/2}}{(1 - a\theta) \left(1 + \frac{\psi}{\psi_0}\right)^n} \right)^{1/m} - 1 \right) / b(s^2 + \sigma^2)^{1/2} \right\}. \quad (24)$$

In writing these equations we have set  $\ell_1 = \ell_2 = \ell_3 = \ell$  since no information is currently available on their relative magnitudes. This was also done by WRIGHT and BATRA [1987] and by BATRA [1987]. Note that in the energy equation, all of the plastic working is taken to be converted into heat.

We presume that the specimen is placed in a hard insulated loading device so that the velocity is prescribed on its top and bottom surfaces. With the origin of the rectangular Cartesian system of axes located at the center of the specimen, we seek solutions of the governing equations which exhibit the following properties.

$$\begin{aligned}
 v(-y,t) &= -v(y,t), & \theta(-y,t) &= \theta(y,t), & \psi(-y,t) &= \psi(y,t), \\
 s(-y,t) &= s(y,t), & \sigma(-y,t) &= -\sigma(y,t).
 \end{aligned}
 \tag{25}$$

Thus the problem for the upper half of the block will be solved under the following boundary conditions.

$$\begin{aligned}
 v(1,t) &= 1, & \theta_{,y}(1,t) &= 0, & \sigma(1,t) &= 0, \\
 v(0,t) &= 0, & \theta_{,y}(0,t) &= 0, & \sigma(0,t) &= 0.
 \end{aligned}
 \tag{26}$$

Figure 1 depicts a solution of eqns (19) through (24), (26), the initial conditions

$$v(y,0) = y, \quad \theta(y,0) = \sigma(y,0) = s(y,0) = \psi(y,0) = 0
 \tag{27}$$

and

$$\begin{aligned}
 \rho &= 3.928 \times 10^{-5}, & k &= 3.978 \times 10^{-3}, & a &= 0.4973, & \mu &= 240.3, \\
 n &= 0.09, & \psi_0 &= 0.017, & b &= 5 \times 10^6, & m &= 0.025.
 \end{aligned}
 \tag{28}$$

The aforementioned values of various parameters are for a typical steel, the average applied strain-rate of  $500 \text{ sec}^{-1}$ , and  $H = 2580 \text{ }\mu\text{m}$ . However, we have taken a rather large value of the thermal softening coefficient  $a$  to reduce the computational effort required to simulate the formation of a shear band. The chosen value of  $a$  gives the nondimen-

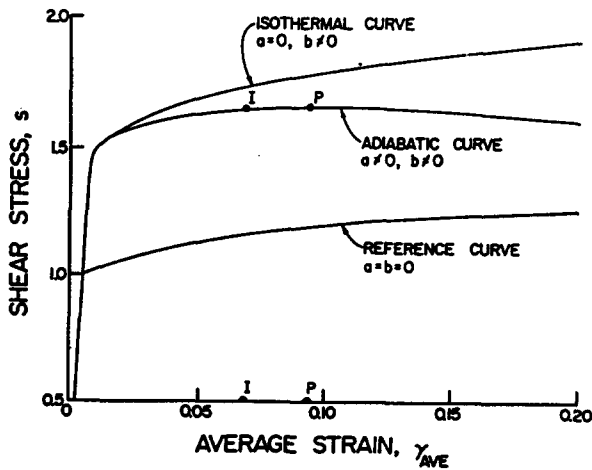


Fig. 1. Average shear stress–average shear strain curve for a typical steel at a nominal strain-rate of  $500 \text{ sec}^{-1}$ .

sional melting temperature to be 2.011. For homogeneous deformations of the block,  $\sigma \equiv 0$ , and the peak (marked as point  $P$  in Fig. 1) in the shear stress-shear strain curve occurs at a strain of 0.093. The uniform temperature  $\theta_0 = 0.1003$  in the block when  $\gamma = 0.0692$ , corresponding to point I in Fig. 1 is perturbed by *adding* a smooth temperature bump

$$\bar{\theta}(y) = 0.1(1 - y^2)^9 e^{-5y^2},$$

and the initial-boundary-value problem described by equations (19)–(24), (26), and the initial conditions

$$\begin{aligned} v(y,0) &= y, \quad \sigma(y,0) = 0, \quad \psi(y,0) = 0.1, \\ \theta(y,0) &= 0.1003 + 0.1(1 - y^2)^9 e^{-5y^2}, \\ s(y,0) &= \left(1 + \frac{0.1}{\psi_0}\right)^n (1 - a\theta(y,0))(1 + b)^m \end{aligned} \quad (29)$$

is solved numerically by using the Galerkin-Gear method. The Galerkin method is used to reduce the partial differential equations to coupled nonlinear ordinary differential equations which are then integrated by using the Gear method for stiff differential equations (GEAR [1971]). We used the subroutine LSODE, taken from the package ODEPACK, developed by HINDMARSH [1983], and employed the option of using the full Jacobian matrix.

### III. COMPUTATION AND DISCUSSION OF RESULTS

Guided by the work of WRIGHT and WALTER [1987] on rigid/visco-plastic materials, we selected a finite element mesh with coordinates of node points given by

$$y_n = \left(\frac{n-1}{160}\right)^p \quad 1 \leq n \leq 161,$$

and computed results for  $p = 3, 5, 7$  on the Floating Point System machine. We tested these meshes on the problem analyzed by Wright and Walter and obtained results virtually identical to their findings. This assured us of the accuracy of the code and the adequacy of the finite element meshes used. All three meshes gave results which were essentially indistinguishable from each other. We first present and discuss results for nonpolar ( $\ell = 0.0$ ) materials and then for dipolar materials with  $\ell = 0.01$ .

#### III.1 Nonpolar materials

For homogeneous deformations of the block, the peak in the shear stress-shear strain curve occurs at an average strain of 0.093. The temperature perturbation (29) was introduced when the block had undergone deformations corresponding to point I in Fig. 1 and the resulting initial-boundary-value problem was solved. We recall that (BATRA

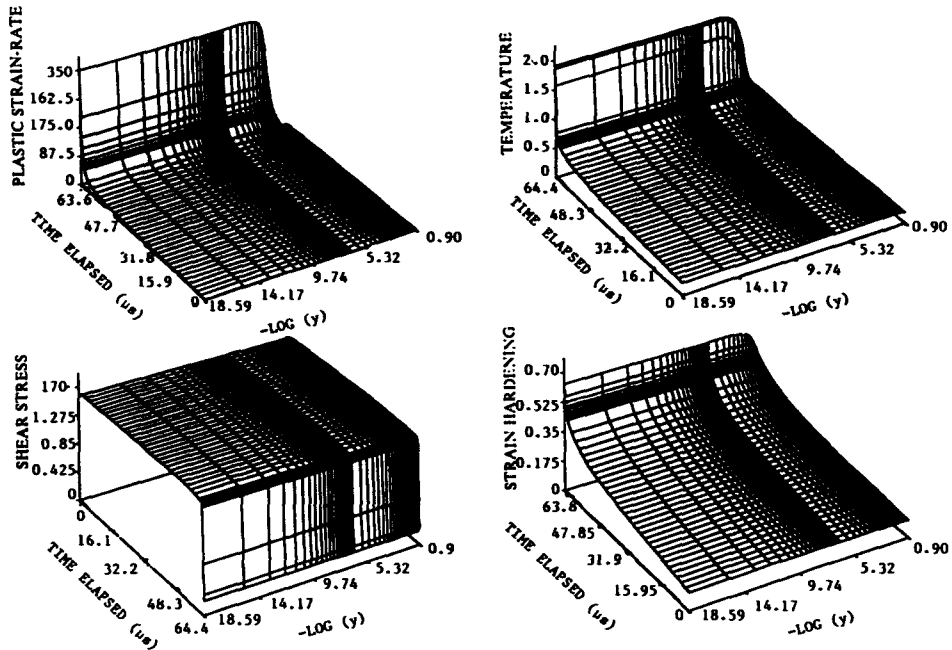


Fig. 2. Evolution of the shear stress, plastic strain-rate, temperature and work-hardening parameter at points near the center of the specimen for nonpolar materials.

[1987]) the average strain at which the deformation begins to localize depends upon, among other factors, the size and the shape of the temperature perturbation. Figure 2 shows the evolution of the shear stress, plastic strain-rate, the temperature and the work-hardening parameter  $\psi$ . Initially, the temperature, plastic strain-rate and the work hardening parameter  $\psi$  increase slowly, and the values of the temperature and  $\psi$  at a point differ approximately by the magnitude of the initial temperature bump. When the average strain in the block equals 0.1002 the rate of increase of the plastic strain rate at points near the center of the block rises sharply and shoots up at an average strain of 0.1011. Thus, for the present problem, the localization of the deformation begins in earnest at an average strain close to 0.1011.

Figure 3 shows the evolution of the plastic strain-rate and the shear stress during the time the severe localization of the deformation is occurring. It is clear from these plots that the shear stress drops to essentially zero in nearly one micro-second even when the strain-hardening effects are included. The shear stress stayed uniform throughout the specimen prior to the initiation of the localization, and during the initial stages of the sudden collapse. But it became nonuniform during the time the localization of the deformation was in progress. This prompted us to examine the field variables more closely.

Figure 4 depicts the distribution of the shear stress and the particle velocity within the specimen at intervals of one-tenth of a microsecond starting with the time when the deformation begins to localize. It is clear that an unloading elastic shear wave emanates outwards from the region of severe deformation. The emanation of the elastic unloading wave is probably associated with the sudden collapse of the shear stress within the band. The computed speed, 3178 m/sec, of the wave essentially equals  $(\mu/\rho)^{1/2}$ , since

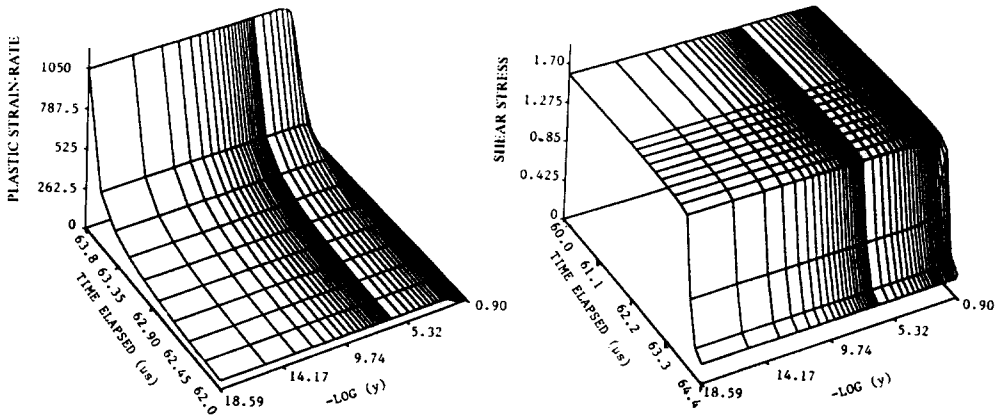


Fig. 3. Collapse of the shear stress and rise of the plastic strain-rate during the localization of the deformation for nonpolar materials.

$$\sqrt{\frac{\mu}{\rho}} = \left( \frac{80 \times 10^9}{7860} \right)^{1/2} = 3,190 \text{ m/sec.}$$

It takes  $0.807 \mu\text{s}$  for the shear wave to reach the outer boundary from which it is reflected back with a negative value of the shear stress. The numerical calculations were not pursued any further.

Figures 5 and 6 depict, at different times, the particle velocity, temperature, plastic strain-rate, work-hardening parameter  $\psi$ , and the shear stress within the region of localization. These results show that the calculations stay stable throughout the severe localization of the deformation. The plots of the plastic strain-rate and  $\psi$  vs.  $y$  at different times indicate that the region of severe deformation becomes smaller with time. Even though the values of  $\psi$  at points near the center of the specimen keep on increasing monotonically, those of  $\dot{\gamma}_p$  begin to oscillate. A possible explanation for this is that

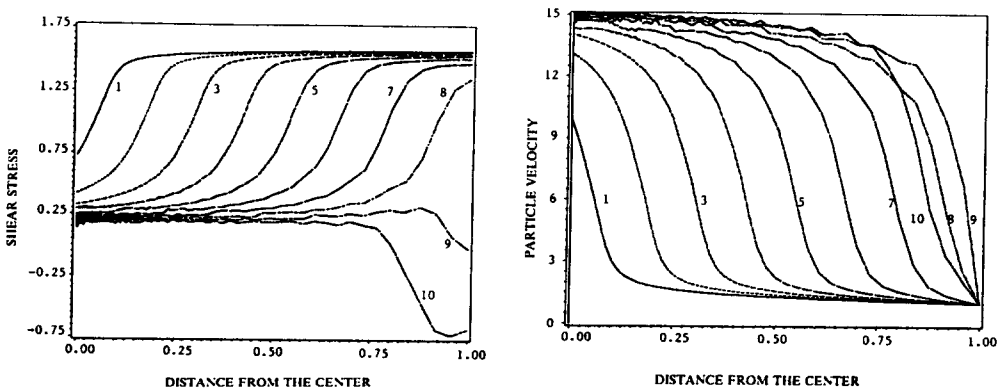


Fig. 4. Distribution of the shear stress and the particle velocity within the specimen at different times during the localization of the deformation for nonpolar materials. These curves are plotted at intervals of  $0.1 \mu\text{s}$  with curve 1 at  $t = 64.0 \mu\text{s}$ , curve 2 at  $t = 64.1 \mu\text{s}$ , curve 3 at  $t = 64.2 \mu\text{s}$ , . . . , and curve 10 at  $t = 64.9 \mu\text{s}$ .

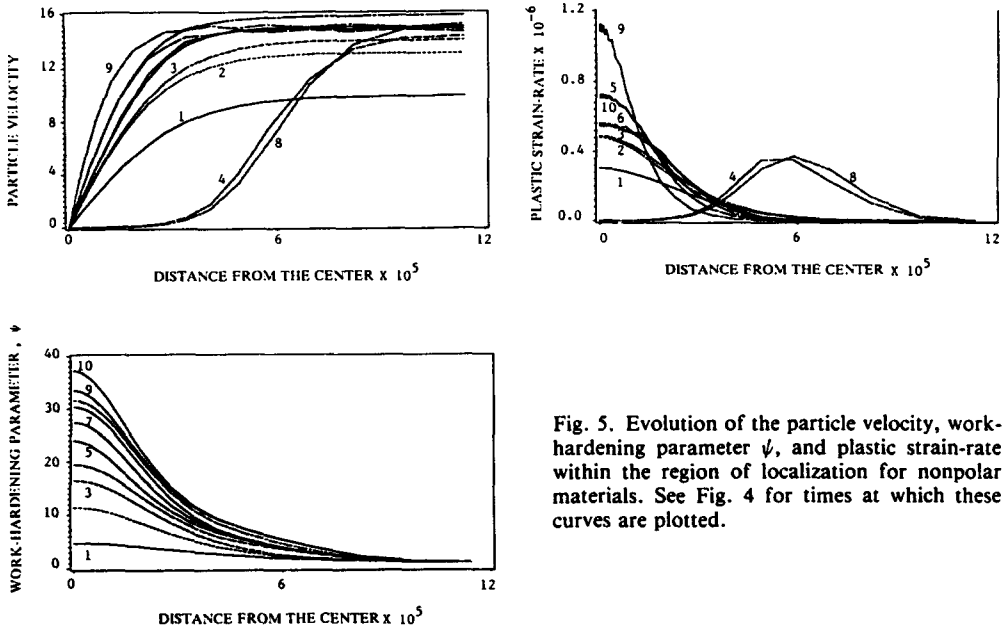


Fig. 5. Evolution of the particle velocity, work-hardening parameter  $\psi$ , and plastic strain-rate within the region of localization for nonpolar materials. See Fig. 4 for times at which these curves are plotted.

there is a diffusive term present in the energy equation, but there is no such term in the equation representing the evolution of  $\psi$  with time. Because of the sharp temperature gradients at points near the center of the specimen, the rate of heat conducted out of the region of localization is high and at times balances the rate of heat generation due to plastic working. When this happens, the softening of the material caused by the rise in its temperature cannot overcome the hardening due to the increase in the value of  $\psi$  and the plastic strain at that material point drops significantly. This in turn reduces the shear stress required for the material to deform plastically because of the reduced hardening due to plastic strain-rate effects. Hence the plastic strain rate begins to increase again

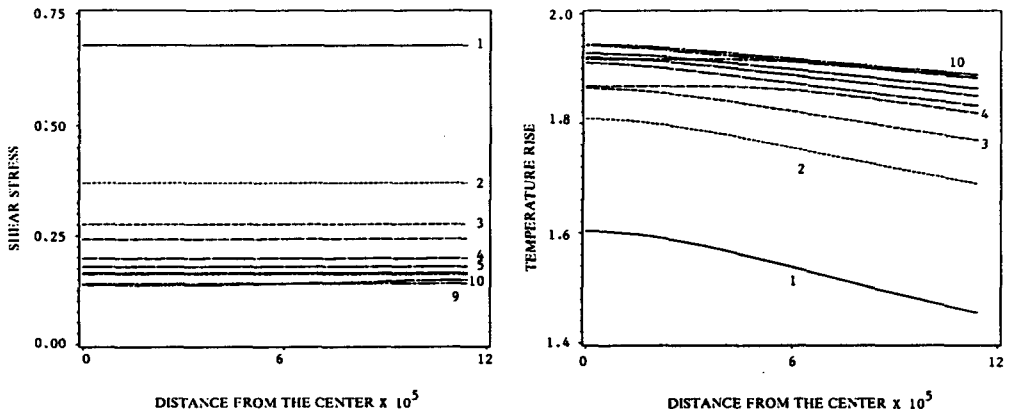


Fig. 6. Evolution of the shear stress and temperature within the region of localization for nonpolar materials. See Fig. 4 for times at which these curves are plotted.

and the phenomenon is repeated though not with any periodicity. The nondimensional plastic strain-rate drops at the center by nearly four-tenth of a million during each one-tenth of a micro-second beginning at  $t = 64.2 \mu\text{s}$ ,  $64.6 \mu\text{s}$  and  $64.8 \mu\text{s}$ .

We now try to write the preceding explanation in the form of an equation. During the time the localization of the deformation is progressing, it is reasonable to assume that material particles near the center of the specimen are deforming plastically. Equation (17) then gives

$$d\dot{\gamma}_p = \frac{(b^{-1} + \dot{\gamma}_p)}{m} \left[ \frac{ds}{s} + \frac{ad\theta}{1 - a\theta} - \frac{nd\psi}{\psi_0 + \psi} \right].$$

Note that  $ds < 0$ ,  $d\theta > 0$  and  $d\psi > 0$ . Therefore, if the middle term on the right-hand side is not larger than the sum of the magnitudes of the other two terms,  $d\dot{\gamma}_p$  will be negative. If the effect of work hardening is neglected, then the relative temperature rise has to overcome the relative drop in stress for  $d\dot{\gamma}_p$  to be positive.

We note that when the shear stress begins to collapse, the temperature at the center of the band equals 76.9% of the presumed melting temperature of the material. It rises to 96% of the melting temperature within  $0.9 \mu\text{sec}$  and then increases extremely slowly. MARCHAND and DUFFY [1988] estimated the maximum temperature within the shear band to be nearly 75% of the melting temperature of the structural steel tested. Since there is no failure or fracture criterion included herein, our calculations may have been carried too far in time.

One possible way to define the width of a shear band is to equate it to the width of the severely deformed region when the unloading elastic wave emanates outwards from this region. This definition gives the width of the shear band for the material model being studied here to be  $0.6 \mu\text{m}$  which does not compare well with those observed experimentally. The difference between the computed and the observed values could be due to the choice of the values of the material parameters and/or the constitutive relations used. The inclusion of nonlocal effects, as discussed below, does increase the width of the severely deformed region.

### III.2 Dipolar materials

In Fig. 7 is plotted the evolution of the shear stress  $s$ , the dipolar stress  $\sigma$ , the temperature change  $\theta$  and the plastic strain-rate  $\dot{\gamma}_p$  when  $\ell$  is set equal to 0.01. Now the shear stress drops gradually rather than suddenly, and the plastic strain rate does not attain the enormously high values it achieved for nonpolar materials. Also the localization of the deformation is delayed considerably as compared to that for nonpolar materials. At points where the magnitude of the gradient of the dipolar stress is maximum, the shear stress attains minimum values. Since  $F \equiv (s - \ell\sigma_{,y})$  acts as a flux for the linear momentum and  $s_e \equiv (s^2 + \sigma^2)^{1/2}$  as the effective stress for determining whether the material particle is deforming elastically or plastically, we have plotted these in Fig. 8. As for the nonpolar case, the flux  $F$  of the linear momentum stays uniform throughout the block and drops in value first gradually and later on rather sharply. The sharp drop in  $F$  is associated with the rapid heating of the material during the final stages of the localization of the deformation. Because of the assumption  $\sigma(0, t) = 0$ ,  $s_e = s$  at the center and, therefore,  $s_e$  drops noticeably at the center due to the softening of the material caused by the rise in temperature. The negative values of  $\sigma$  imply that  $d_p$  exceeds  $v_{,yy}$ . The

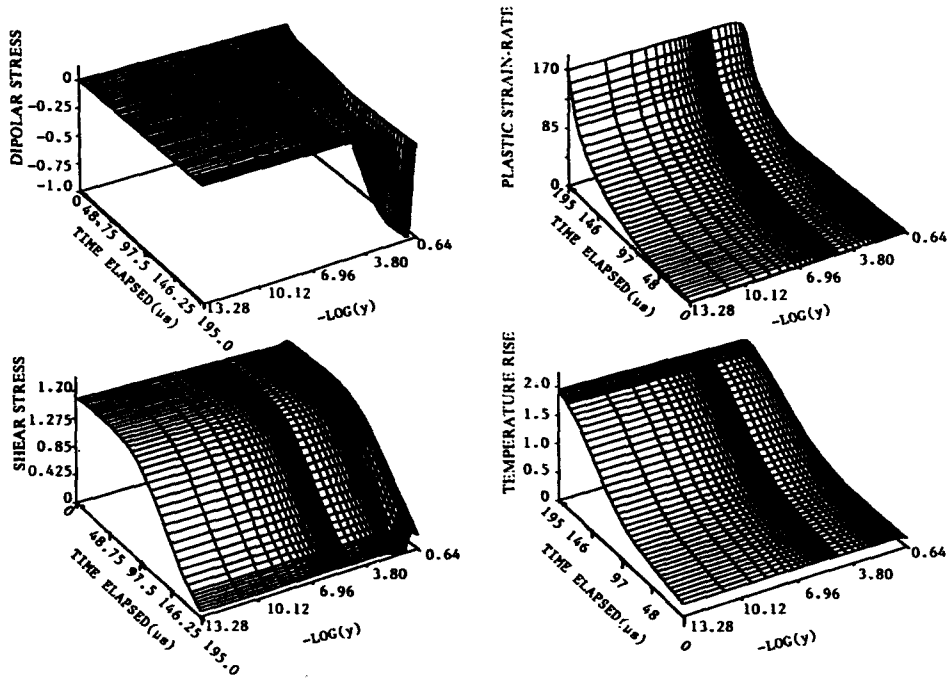


Fig. 7. Evolution of the shear stress, dipolar stress, temperature and plastic strain-rate at points near the center of the specimen for dipolar materials with  $\ell = 0.01$ .

larger values of  $|\sigma|$  at points away from the center make the effective stress  $s_e$  bigger there. The point where  $s_e$  assumes maximum values moves towards the center of the block as the deformation proceeds but becomes stationary when the deformation begins to localize severely. In Figs. 9 and 10 we have plotted the distribution of the particle

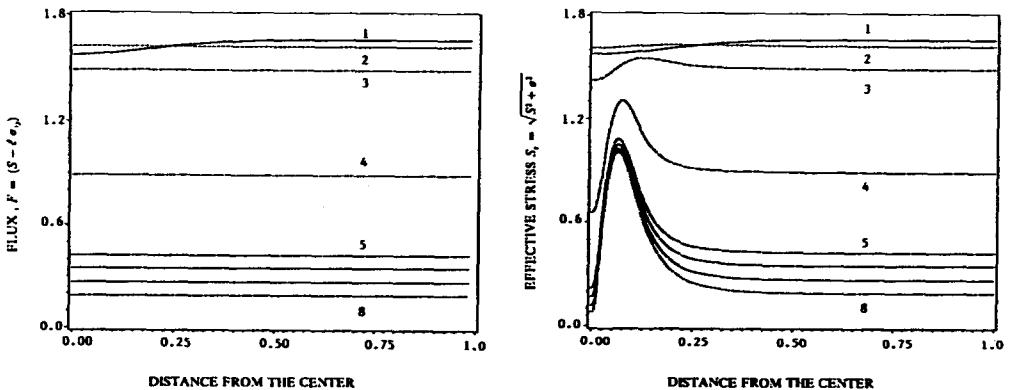


Fig. 8. Distribution of the flux of the linear momentum and the effective stress within the specimen at different times during the localization of the deformation for dipolar materials. Times for the plot of these results are: curve 1,  $t = 0.0 \mu s$ ; curve 2,  $t = 50 \mu s$ ; curve 3,  $t = 100 \mu s$ ; curve 4,  $t = 150 \mu s$ ; curve 5,  $t = 180 \mu s$ ; curve 6,  $t = 185 \mu s$ ; curve 7,  $t = 190 \mu s$ ; curve 8,  $t = 195 \mu s$ .

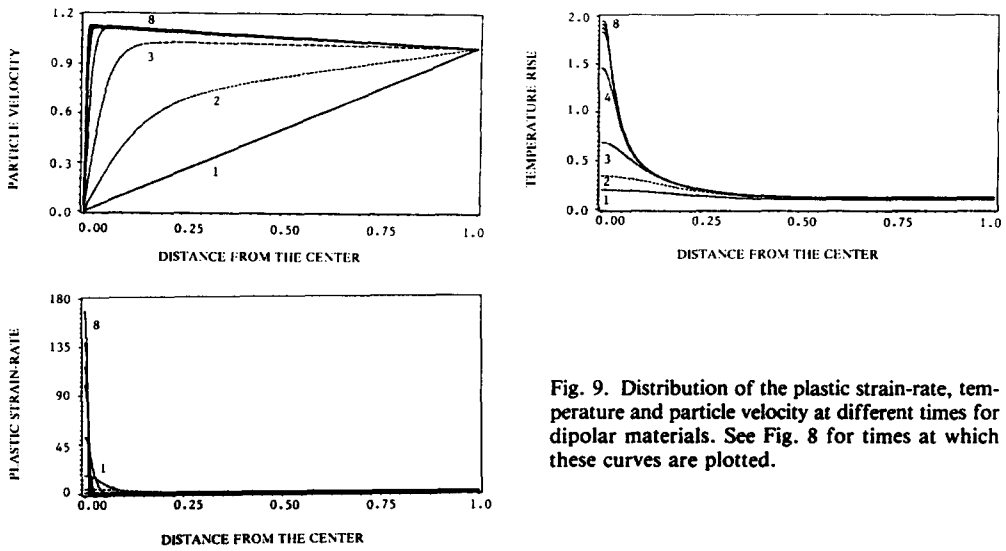


Fig. 9. Distribution of the plastic strain-rate, temperature and particle velocity at different times for dipolar materials. See Fig. 8 for times at which these curves are plotted.

speed, temperature, plastic strain-rate,  $s$  and  $\sigma$  within the specimen at different times. It is obvious that there is no unloading wave emanating outwards from the severely deformed region. This is to be expected since the governing equations for  $l \neq 0$  do not have real characteristics. The particle speed increases from the prescribed value of zero at the center of the specimen to 1.14 at the edge of the severely deformed region, and then almost linearly to the prescribed value of 1.0 at the outer boundary of the specimen. The temperature and the plastic strain-rate at the center continue to increase.

In order to decipher the details of the deformation at points near the center of the specimen, we have plotted in Figs. 11 and 12 several field variables within  $0 < y < 0.10$  and at different times. These figures show vividly that the temperature and the work-hardening parameter have attained steady values at points for which  $0.0175 < y < 0.10$ .

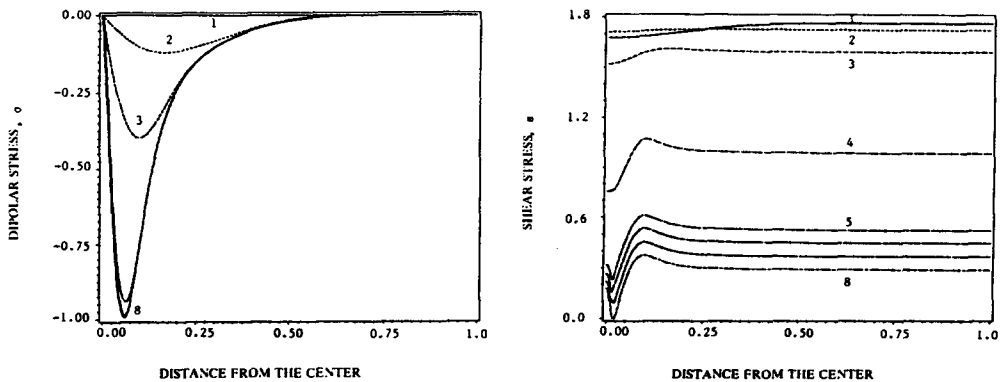


Fig. 10. Distribution of the shear stress and the dipolar stress at different times for dipolar materials. See Fig. 8 for times at which these curves are plotted.

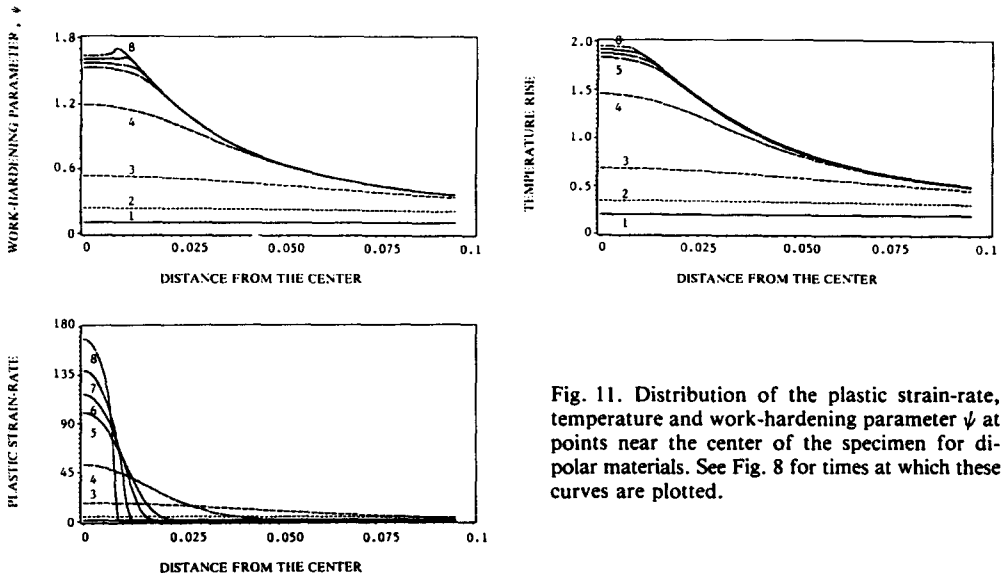


Fig. 11. Distribution of the plastic strain-rate, temperature and work-hardening parameter  $\psi$  at points near the center of the specimen for dipolar materials. See Fig. 8 for times at which these curves are plotted.

The shear stress continues to drop and is minimum not at the center but at a point slightly away from it. The temperature at points near the center of the block continues to rise and has essentially uniform values in the region  $0 \leq y \leq 0.01$ . Even though the shear stress at some points becomes negative for  $t \geq 190 \mu\text{sec}$ , the flux  $F$  of linear momentum is still positive throughout the block. Up to the time these computations have been performed, the peak temperature has not reached the presumed value 2.011 of the melting point of the material. Since the severely deforming region is still narrowing down, it is unclear as to how to define the band width or when to stop the numerical computations for the dipolar case. One possibility is to end the computations when  $s$  at any point in the domain becomes zero and regard the width of the severely deformed region as equal to the band width. According to this criterion, the width of the heavily

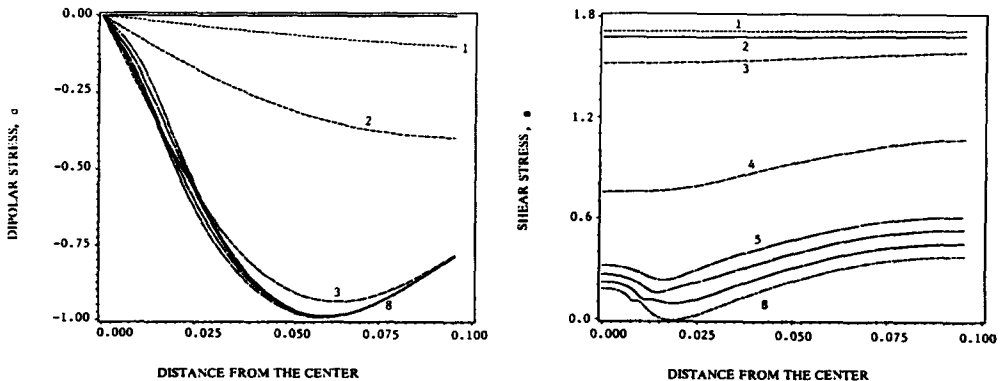


Fig. 12. Distribution of the shear stress and dipolar stress at points near the center of the specimen. See Fig. 8 for times at which these curves are plotted.

deformed region, computed for  $t = 190 \mu\text{s}$ , equals  $2 \times 0.0129 \times 2580 = 66.4 \mu\text{m}$ . This value is close to those observed experimentally, but the experimentally observed (MARCHAND & DUFFY [1988]) quick drop of the shear stress is not predicted by the dipolar theory. Since the value of  $\ell$  was arbitrarily chosen to be 0.01, there is some room for adjustment. WRIGHT and BATRA [1987] did compute results for  $\ell = 0.001$ , but the calculations were not carried far enough in time.

BATRA and KIM [1988], using the present material model, have computed results for  $\ell = 0.005$ , 0.001 and 0.0005. Their computations show that as  $\ell$  is decreased from 0.01 to 0.0005, the computed band width decreases from  $66.4 \mu\text{m}$  to  $1.0 \mu\text{m}$ , the maximum plastic strain-rate at the center increases from 139 to 99,606, and the average strain when the shear stress first becomes zero decreases from 0.1642 to 0.1023. There was no unloading elastic wave observed for any of these three values of the material characteristic length  $\ell$ .

#### IV. CONCLUSIONS

It is shown that when the uniform temperature field in an elastic/viscoplastic block undergoing simple shearing deformations is perturbed, the deformation localizes. During the localization of the deformation, the stress collapses quickly for nonpolar materials but decreases to zero gradually for dipolar materials. For nonpolar materials, the sharp drop of the shear stress in the narrow region undergoing severe deformations results in an elastic unloading wave to travel outwards from this region to the outer boundaries of the specimen. Both for dipolar and nonpolar materials the temperature and the work hardening parameter continue to increase. Whereas, for dipolar materials, the plastic strain-rate keeps on increasing within the region of the localized deformation; for nonpolar materials, the plastic strain rate oscillates indicating the competing effects of thermal softening and hardening due to plastic strain and plastic strain-rate.

*Acknowledgements*—R.C. Batra is grateful to Drs. T.W. Wright and John Walter, Jr., of the Ballistic Research Laboratory for helpful discussions on the subject. This work was supported by the U.S. National Science Foundation grant MSM 8715952, and the U.S. Army Research Office Contracts DAAG29-85-K-0238 and DAAL03-88-K-0184 to the University of Missouri-Rolla.

#### REFERENCES

- 1944 ZENER, C. and HOLLomon, J.H., "Effect of Strain Rate on Plastic Flow of Steel," *J. Appl. Phys.*, **15**, 22.
- 1968 GREEN, A.E., McINNIS, B.C., and NAGHDI, P.M., "Elastic-Plastic Continua with Simple Force Dipole," *Int. J. Eng. Sci.*, **6**, 373.
- 1971 GEAR, C.W., "Numerical Initial Value Problems in Ordinary Differential Equations," Prentice-Hall, Englewood Cliffs, New Jersey.
- 1977 LITONSKI, J., "Plastic Flow of a Tube Under Adiabatic Torsion," *Bull. Acad. Pol. Sci.*, **25**, 7.
- 1979 ROGERS, H.C., "Adiabatic Plastic Deformation," *Ann. Rev. Mat. Sci.*, **9**, 23.
- 1983 HINDMARSH, A.C., "ODEPACK, A Systematized Collection of ODE Solvers," in STEPLEMAN, R.S. *et al.* (Ed.), *Scientific Computing*, North-Holland, Amsterdam, pp. 55-64.
- 1983 ROGERS, H.C., "Adiabatic Shearing—General Nature and Material Aspects," in MEXALL, J. and WEISS, V. (Eds.) *Material Behavior Under High Stress and Ultrahigh Loading Rates*, Plenum Press, New York, pp. 101-118.
- 1984 CLIFTON, R.J., DUFFY, J., HARTLEY, K.A., and SHAWKI, T.G., "On Critical Conditions for Shear Band Formation at High Strain Rates," *Scripta Metallurgica*, **18**, 443.
- 1984 MALVERN, L. in HARDING, J. (Ed.) *Mechanical Properties at High Rates of Strain*, Inst. Physics, Bristol and London, pp. 1-20.
- 1985 COLEMAN, B.D. and HODGDON, M.L., "On Shear Bands in Ductile Materials," *Arch. Rational Mech. Anal.*, **90**, 219.

- 1985 WRIGHT, T.W. and BATRA, R.C., "The Initiation and Growth of Adiabatic Shear Bands," *Int. J. Plasticity*, **1**, 205.
- 1987 BATRA, R.C., "The Initiation and Growth of, and the Interaction Among, Adiabatic Shear Bands in Simple and Dipolar Materials," *Int. J. Plasticity*, **3**, 75.
- 1987 WRIGHT, T.W. and BATRA, R.C., "Adiabatic Shear Bands in Simple and Dipolar Plastic Materials" in KAWATA, K. and SHIOIRI, J. (Eds.) *Proc. IUTAM Symposium on Macro- and Micro-Mechanics of High Velocity Deformation and Fracture*, Springer-Verlag, Berlin-Heidelberg-New York, pp. 189-201.
- 1987 WRIGHT, T.W. and WALTER, J.W., "On Stress Collapse in Adiabatic Shear Bands," *J. Mech. Phys. Solids*, **35**, 701.
- 1988 BATRA, R.C. and KIM, C.H., "Effect of Material Characteristic Length on the Initiation, Growth, and Band Width of Adiabatic Shear Bands in Dipolar Materials," *J. de Physique*, **49(C3)**, 41.
- 1988 MARCHAND, A. and DUFFY, J., "An Experimental Study of the Formation of Adiabatic Shear Bands in a Structural Steel," *J. Mech. Phys. Solids*, **36**, 251.

Department of Mechanical and Aerospace Engineering and Engineering Mechanics  
University of Missouri-Rolla  
Rolla, MO 65401-0249

*(Received 22 June 1988; in final revised form 29 October 1988)*